10.24425/acs.2023.145117

Archives of Control Sciences
Volume 33(LIX), 2023
No. 1, *pages 127–153*

Bifurcation analysis, circuit design and sliding mode control of a new multistable chaotic population model with one prey and two predators

Sundarapandian VAIDYANATHAN, Khaled BENKOUIDER,
Aceng SAMBAS and P. DARWIN

In this work, we report a new chaotic population biology system with one prey and two predators. Our new chaotic population model is derived by introducing two nonlinear interaction terms between the prey and predator-2 to the Samardzija-Greller population biology system (1988). We show that the new chaotic population biology system has a greater value of Maximal Lyapunov Exponent (MLE) than the Maximal Lyapunov Exponent (MLE) of the Samardzija-Greller population biology system (1988). We carry out a detailed bifurcation analysis of the new chaotic population biology system with one prey and two predators. We also show that the new chaotic population biology model exhibits multistability with coexisting chaotic attractors. Next, we use the integral sliding mode control (ISMC) for the complete synchronization of the new chaotic population biology system with itself, taken as the master and slave chaotic population biology systems. Finally, for practical use of the new chaotic population biology system, we design an electronic circuit design using Multisim (Version 14.0).

Key words: population biology system, chaos, chaotic systems, synchronization, sliding mode control, Multisim, circuit simulation

S. Vaidyanathan (corresponding author, e-mail: sundarvtu@gmail.com) is with Centre for Control Systems, Vel Tech University, 400 Feet Outer Ring Road, Avadi, Chennai-600092, Tamil Nadu, India.

K. Benkouider (e-mail: benkouider.khaled@gmail.com) is with Non Destructive Testing Laboratory, Automatic Department, Jijel University, BP 98, 18000, Jijel, Algeria.

A. Sambas (e-mail: acengs@umtas.ac.id) is with Department of Mechanical Engineering, Universitas Muhammadiyah Tasikmalaya, Tasikmalaya 46196, West Java, Indonesia.

P. Darwin (e-mail: darwin.p@ritchennai.edu.in) is with Department of Computer Science and Engineering, Rajalakshmi Institute of Technology, Kuthambakkam, Chennai-600 124, Tamil Nadu, India.

Received 28.09.2022. Revised 11.01.2023.

1. Introduction

Chaotic systems have many applications due to their complexity [1]. Memristors [2–4], circuits [5, 6], neural networks [7, 8] and cybersecurity [9, 10] are some well-known areas where chaotic systems are applied in practice.

A two-species population biology system describing the interaction between a predator and a prey, popularly called as the predator-prey model was developed independently by A.J. Lotka ([11], 1925) and V. Volterra ([12], 1926). Samardzija and Greller ([13], 1988) generalized the two-species Lotka-Volterra model to derive a chaotic population biology system with two preys and one predator in which two quadratic nonlinearities and two cubic nonlinearities were used for the interactions of the predators with the prey. Using active nonlinear control, Agrawal et al. ([14], 2012) derived results for the asymptotic synchronization between Ravinovich–Fabrikant chaotic system [15] and Samardzija-Greller chaotic system [13]. Kocamaz et al. ([16], 2020) designed a sliding mode controller to stabilize the states of the Samardzija-Greller chaotic system [13].

In this work, we report a new chaotic population biology system with one prey and two predators. Our new chaotic population model is derived by introducing two nonlinear interaction terms between the prey and predator-2 to the Samardzija-Greller population biology system [13]. We show that the new chaotic population biology system has a greater value of positive Lyapunov component than that of the Samardzija-Greller population biology system (1988). We also show that the new chaotic population biology system has a greater value of Kaplan-Yorke dimension than that of the Samardzija-Greller population biology system [13]. These calculations pinpoint that the new chaotic population model exhibits more complexity than the Samardzija-Greller population biology system [13].

Bifurcation analysis of chaotic systems yields useful information about the dynamic properties of the systems as we vary the parameters of the systems [17, 18]. We carry out a detailed bifurcation analysis of the new chaotic population biology system with one prey and two predators. We also establish that the new chaotic population biology system exhibits multistability with coexisting chaotic attractors. Multistability refers to the phenomenon of coexistence of periodic or chaotic attractors for a nonlinear dynamical system for the same set of system parameters but various values of the initial states of the dynamical system [19, 20].

Next, we use integral sliding mode control (ISMC) for the complete synchronization of the new chaotic population biology system with itself, taken as the master and slave chaotic population biology systems. In the integral sliding mode control, the system motion under ISMC has a dimension equal to that of the state space. In ISMC, the system trajectory always starts from the sliding surface. Thus, the reaching phase is eliminated in ISMC, and robustness in the whole state space is achieved. ISMC is a popular control technique used in many engineering appli-

cations [21–23]. Finally, we design an electronic circuit design using MultiSim (Version 14.0). Circuit design of chaotic systems is very useful for implementing the chaotic systems under study for practical applications [24, 25].

2. A new chaotic population model with one prey and two predators

A chaotic population biology system with two preys and one predator was proposed by Samardzija and Greller ([13], 1988) with two quadratic nonlinearities and two cubic nonlinearities used for the interactions of the predators with the prey.

Samardzija-Greller 3-species population model [13] is described by the following dynamics:

$$\dot{z}_1 = z_1 - z_1 z_2 + r z_1^2 - p z_1^2 z_3 \,, \tag{1a}$$

$$\dot{z}_2 = -z_2 + z_1 z_2 \,, \tag{1b}$$

$$\dot{z}_3 = -q z_3 + p z_1^2 z_3 \,. \tag{1c}$$

In the 3-species model (1), z_1 is the single prey and z_2, z_3 are the two predators. The nonlinear interactions between the prey and the predator-1 are given by the terms $-z_1 z_2$ in (1a) and $z_1 z_2$ in (1b). The nonlinear interactions between the prey and the predator-2 are given by the terms $-p z_1^2 z_3$ in (1a) and $p z_1^2 z_3$ in (1c). In the population model (1), p, q and r are positive constants, which are called as the Malthusian parameters.

Samardzija and Greller [13] established in their work that the 3-species Lotka-Volterra population model (1) is chaotic when the Malthusian parameters in the model (1) take the following values:

$$p = 2.98, \quad q = 3, \quad r = 7. \tag{2}$$

The chaotic behaviour of the Samardzija-Greller system (1) for the Malthusian parameter values (2) is confirmed by calculating the local Lyapunov exponents for the initial state $Z(0) = (1.4, 1.0, 1.4)$. A numerical estimation in MATLAB gives the local Lyapunov exponents of the Samardzija-Greller system (1) for $(p, q, r) = (2.98, 3, 7)$ and $Z(0) = (1.4, 1.0, 1.4)$ for $T = 1E3$ seconds as follows:

$$\tau_1 = 0.00161, \quad \tau_2 = 0, \quad \tau_3 = -0.01390. \tag{3}$$

The complexity of the Samardzija-Greller system (1) is further estimated by calculating the Kaplan-Yorke dimension of the chaotic population system (1) as follows:

$$D_{KY} = 2 + \frac{\tau_1 + \tau_2}{|\tau_3|} = 2.1158. \tag{4}$$

In this research work, we develop a new 3-species population biology system with one prey and two predators by introducing two nonlinear interaction terms between the prey and predator-2 to the Samardzija-Greller system (1).

Our new population biology model is described by the following 3-D dynamics:

$$\dot{z}_1 = z_1 - z_1 z_2 + r z_1^2 - s z_1 z_3 - p z_1^2 z_3 \,, \tag{5a}$$

$$\dot{z}_2 = -z_2 + z_1 z_2 \,, \tag{5b}$$

$$\dot{z}_3 = -q z_3 + s z_1 z_3 + p z_1^2 z_3 \,. \tag{5c}$$

In the new 3-species model (5), z_1 is the single prey and z_2, z_3 are the two predators. The nonlinear interactions between the prey and the predator-1 are given by the terms $-z_1 z_2$ in (5a) and $z_1 z_2$ in (5b). The nonlinear interactions between the prey and the predator-2 are given by the terms $-s z_1 z_3$, $-p z_1^2 z_3$ in (5a) and $s z_1 z_3$, $p z_1^2 z_3$ in (5c). In the population model (1), p, q, r and s are positive constants, which are called as the Malthusian parameters.

In this research work, we will that the new 3-species Lotka-Volterra population model is chaotic when the Malthusian parameters in the model (5) take the following values:

$$p = 1.8, \quad q = 3, \quad r = 8, \quad s = 0.2. \tag{6}$$

The chaotic behaviour of the new 3-species population biology model (5) for the Malthusian parameter values (6) is confirmed by calculating the local Lyapunov exponents for the initial state $Z(0) = (1.4, 1.0, 1.4)$. A numerical estimation in MATLAB for seconds gives the local Lyapunov exponents of the new population biology model (5) for $(p, q, r, s) = (1.8, 3, 8, 0.2)$ and $Z(0) = (1.4, 1.0, 1.4)$ as follows:

$$\tau_1 = 0.03424, \quad \tau_2 = 0, \quad \tau_3 = -0.03826. \tag{7}$$

The maximal Lyapunov exponent (MLE) of the new population biology model (5) is $\tau_{\max} = 0.03424$, which is larger than the maximal Lyapunov exponent (MLE) of the Samardzija-Greller system (1) given by $\tau_{\max} = 0.00161$.

The complexity of the new 3-species population biology model (5) is further estimated by calculating the Kaplan-Yorke dimension of the new chaotic population system (5) as follows:

$$D_{KY} = 2 + \frac{\tau_1 + \tau_2}{|\tau_3|} = 2.8949. \tag{8}$$

The value of the Kaplan-Yorke dimension of the new chaotic population system (5) is much greater than the value of the Kaplan-Yorke dimension of the

Samardzija-Greller system (1). Hence, we deduce that the new chaotic populations system (5) exhibits more complexity than the Samardzija-Greller system (1).

The phase portraits of the new chaotic population model (5) for the paramater values (6) and $Z(0) = (1.4, 1.0, 1.4)$ are plotted in Figures 1 to 3.

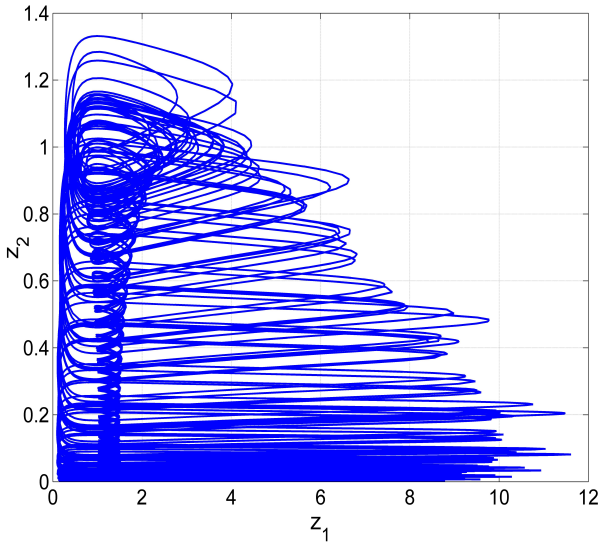

Figure 1: MATLAB phase plot of the new 3-species Lotka-Volterra chaotic population model (5) in (z_1, z_2) plane

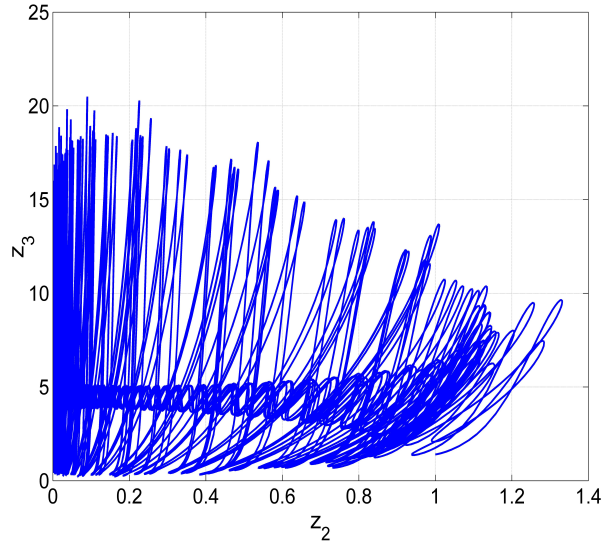

Figure 2: MATLAB phase plot of the new 3-species Lotka-Volterra chaotic population model (5) in (z_2, z_3) plane

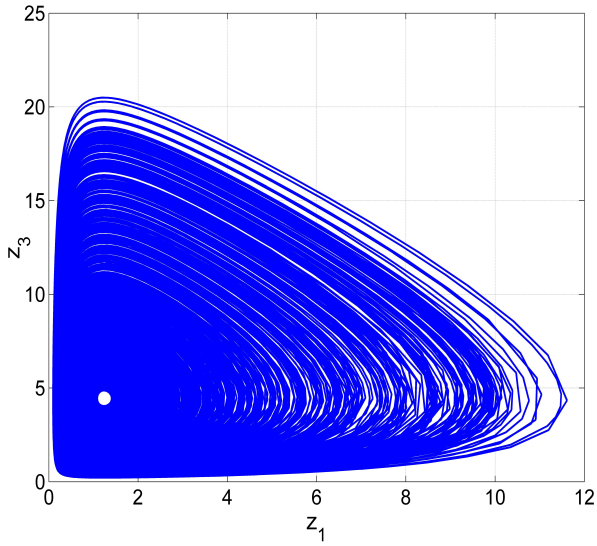

Figure 3: MATLAB phase plot of the new 3-species Lotka-Volterra chaotic population model (5) in (z_1, z_3) plane

3. Bifurcation Study of the New Chaotic Population Model

This section will study the influence of the four parameters on the chaotic properties of the new population biology system (5). We will give a detailed analysis of the new system's behavior including definition of parameters regions wherein system (5) develops weak chaos ($\tau_1 < 0.01$), robust chaos ($\tau_1 > 0.01$), periodic behavior ($\tau_1 = 0$) or stability zone ($\tau_1 < 0$).

3.1. Variation of the parameter p

Here, we fix $q = 3$, $r = 8$, $s = 0.2$ and vary p in the interval $[1.7, 3]$.

Figure 4 represents the LEs spectrum and bifurcation diagram of system (5) when p increases from 1.7 to 3. It demonstrates how sensitive the new population biology system (5) is to variations in the parameter p value.

By examining the LEs and the bifurcation diagram shown in Figure 4, we find that the novel population biology model (5) may experience a set of scenarios, such as robust chaos, weak chaos, periodic behavior, or convergence to a stable state, depending on the value of parameter p.

The new population biology model (5) as illustrated in Figure 4(b) contains one positive LE bigger than 0.01 for $p \in [1.7, 2]$. System (5) has robust chaotic behavior over this range of parameter p, as illustrated in Figure 4(a). We choose a number from this range and set p as follows: $p = 1.7$. This will serve to generate an illustration of the chaotic attractors produced by system (5) when $p \in [1.7, 2]$.

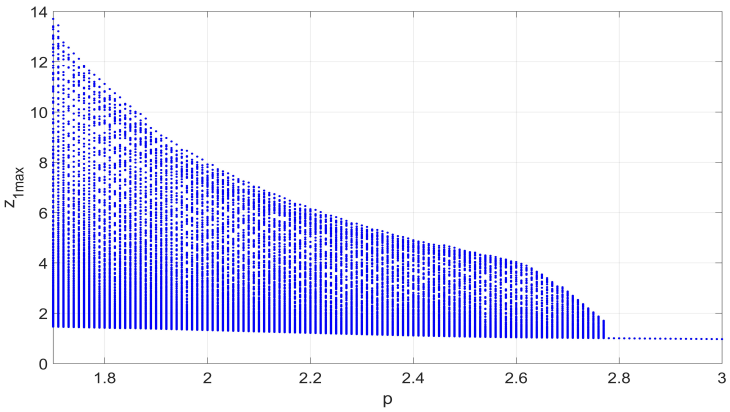

(a)

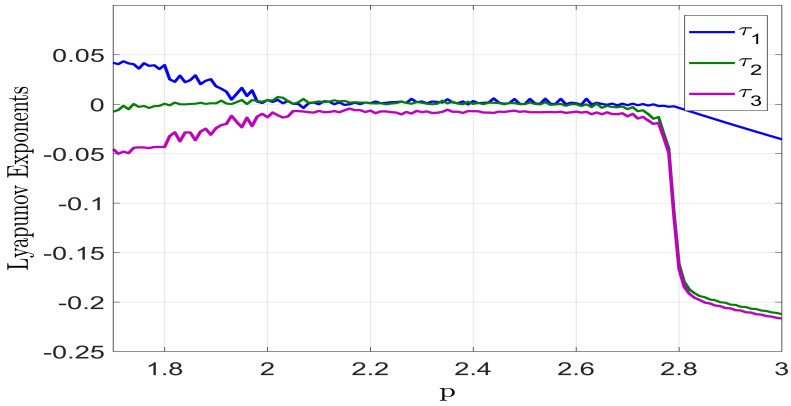

(b)

Figure 4: Dynamic analysis of the new 3-species population biology system (5) when $p \in [1.7, 3]$, $q = 3$, $r = 8$ and $s = 0.2$: (a) Bifurcation diagram and (b) LE spectrum

Then, as shown in Figure 5(a), the (z_1, z_2) chaotic attractor of system (5) is displayed in blue for $p = 1.7$. The associated Lyapunov exponents (LEs) and Kaplan-Yorke dimension (D_{KY}) are:

1) $\tau_1 = 0.042$, $\tau_2 = 0$ and $\tau_3 = -0.045$.

2) $D_{KY} = 2.93$.

As seen in Figure 4(b), the new population biology model (5) has one positive LE smaller than 0.01 for $p \in [2, 2.7]$. Hence, the system (5) exhibits weak chaotic behavior across this parameter p range. We select a value from this range, and we set p to be: $p = 2.44$. The (z_1, z_2) chaotic attractor of the system (5) is then

presented in red for $p = 2.44$ as seen in Figure 5(a). The associated LEs and DKY are as follows:

1) $\tau_1 = 0.006$, $\tau_2 = 0$ and $\tau_3 = -0.009$.

2) $D_{KY} = 2.67$.

The new population biology model (5) contains one zero and two negative LEs for $p \in [2.7, 2.8]$, as can be observed in Figure 5(b). As a result, the system (5) displays periodic behavior across this range of p. In Figure 5(b), the (z_1, z_2)

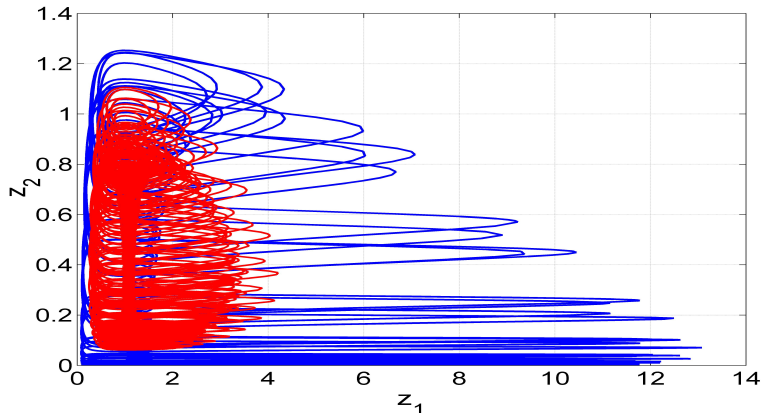

(a)

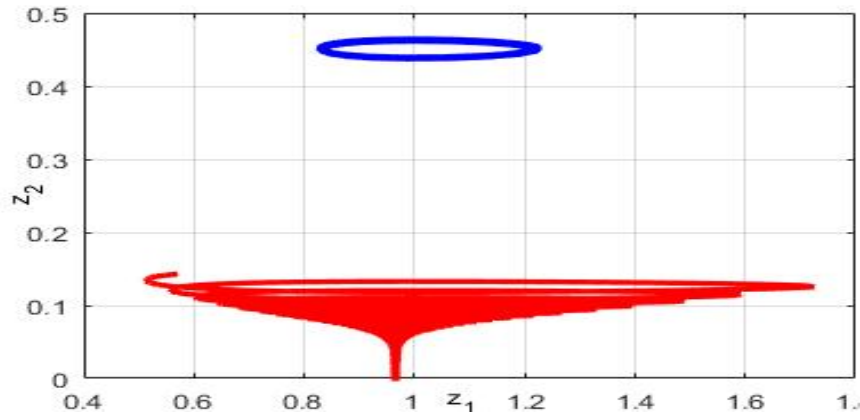

(b)

Figure 5: MATLAB phase portraits of the new population biology system (5) in (z_1, z_2) plane for different values of p: (a) in blue: chaotic attractor ($p = 1.7$), in red: chaotic attractor ($p = 2.44$), and (b) in blue: periodic attractor ($p = 2.75$), in red: Convergence to stable state ($p = 3$)

periodic attractor of the system (5) is shown in blue for $p = 2.75$. The associated LEs and D_{KY} are as follows:

1) $\tau_1 = 0$, $\tau_2 = -0.015$ and $\tau_3 = -0.019$.
2) $D_{KY} = 0$.

Finally, when $p \in [2.8, 3]$, the system (5) has three negative LEs indicating that it converge to its stable state. In Figure 5(b), the convergence of the (z_1, z_2) portrait to stable state of system (5) is shown in red for $p = 3$. The associated LEs and DKY are as follows:

1) $\tau_1 = -0.035$, $\tau_2 = -0.212$ and $\tau_3 = -0.217$.
2) $D_{KY} = 0$.

3.2. Variation of the parameter q

Here, we fix $p = 1.8$, $r = 8$, $s = 0.2$ and vary q in the interval $[1.5, 4.5]$.

Figure 6 represents the LEs spectrum and bifurcation diagram of system (5) when q increases from 1.5 to 4.5. It demonstrates how sensitive the new population biology system (5) is to variations in the parameter q value.

By examining the LEs and the bifurcation diagram shown in Figure 6, we find that the novel population biology model (5) may experience a set of scenarios, such as convergence to a stable state, weak chaos and robust chaos, depending on the value of parameter q.

When $q \in [1.5, 2.1]$, the new population biology model (5) has three negative LEs indicating that it converges to a stable state. In Figure 7 (a), the the convergence of the (z_1, z_3) portrait to stable state of system (5) is shown for $q = 1.5$. The associated Lyapunov exponents (LEs) and Kaplan-Yorke dimension (D_{KY}) are:

1) $\tau_1 = -0.045$, $\tau_2 = -0.052$ and $\tau_3 = -0.153$.
2) $D_{KY} = 0$.

As seen in Figure 6(b), the new population biology model (5) has one positive LE smaller than 0.01 for $q \in [2.1, 2.5]$. Hence, the system (5) exhibits weak chaotic behavior across this parameter q range. We select a value from this range, and we set q to be: $q = 2.44$. The (z_1, z_3) chaotic attractor of the system (5) is then presented in red for $q = 2.44$ as seen in Figure 7 (b). The associated LEs and DKY are as follows:

1) $\tau_1 = 0.009$, $\tau_2 = 0$ and $\tau_3 = -0.025$.
2) $D_{KY} = 2.36$.

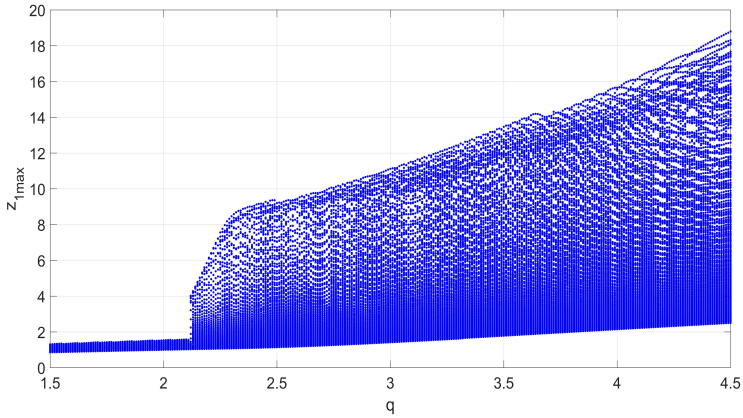

(a)

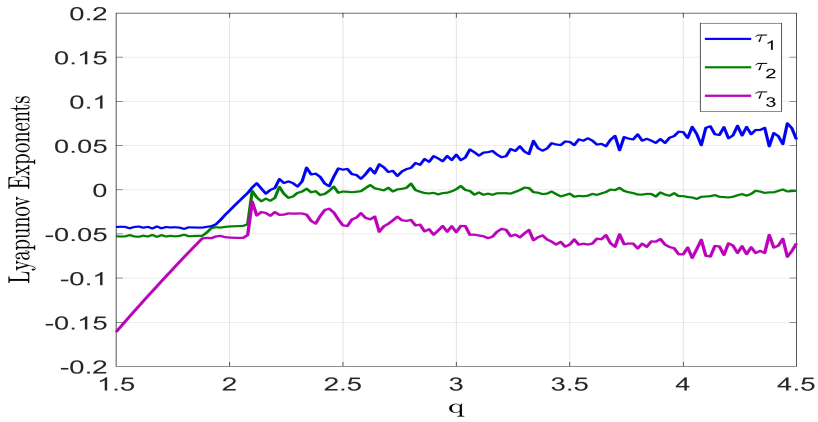

(b)

Figure 6: Dynamic analysis of the new 3-species population biology system (5) when $p = 1.8$, $q \in [1.5, 4.5]$, $r = 8$ and $s = 0.2$: (a) Bifurcation diagram and (b) LE spectrum

As seen in Figure 6(b), the new population biology model (5) has one positive LE bigger than 0.01 for $q \in [2.5, 4.5]$. Hence, the system (5) exhibits robust chaotic behavior across this parameter q range. We select a value from this range, and we set q to be: $q = 4.5$. The (z_1, z_3) chaotic attractor of the system (5) is then presented in blue for $q = 4.5$ as seen in Figure 7(b). The associated LEs and DKY are as follows:

1) $\tau_1 = 0.065$, $\tau_2 = 0$ and $\tau_3 = -0.066$.

2) $D_{KY} = 2.98$.

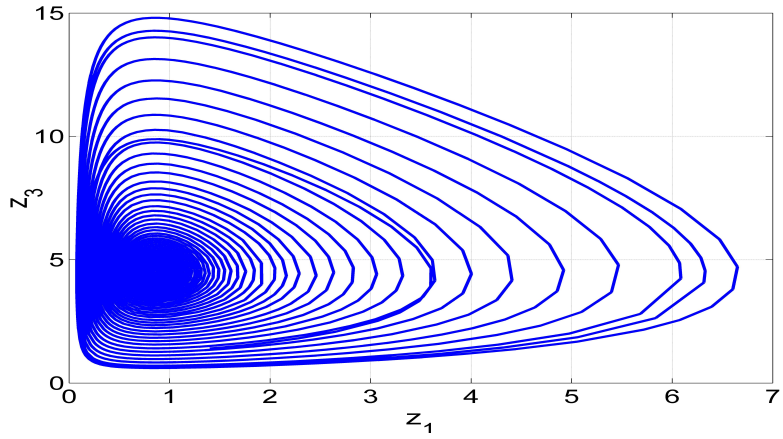

(a)

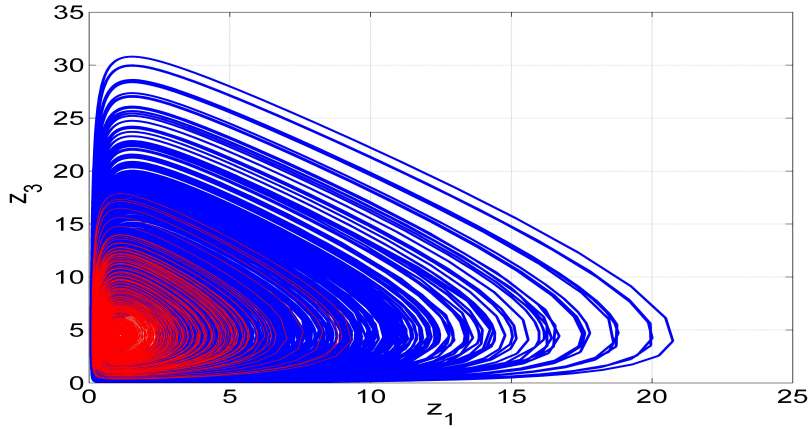

(b)

Figure 7: MATLAB phase portraits of the new population biology system (5) in (z_1, z_3) plane for different values of q: (a) Convergence to stable state ($q = 1.5$) and (b) in blue: chaotic attractor ($q = 4.5$), in red: chaotic attractor ($q = 2.44$)

3.3. Variation of the parameter r

Here, we fix $p = 1.8$, $q = 3$, $s = 0.2$ and vary r in the interval $[1, 8]$.

Figure 8 represents the LEs spectrum and bifurcation diagram of system (5) when r increases from 1 to 8. It demonstrates how sensitive the new population biology system (5) is to variations in the parameter r value.

By examining the LEs and the bifurcation diagram shown in Figure 8, we find that the novel population biology model (5) may experience a set of scenarios,

such as convergence to a stable state, weak chaos and robust chaos, depending on the value of parameter r.

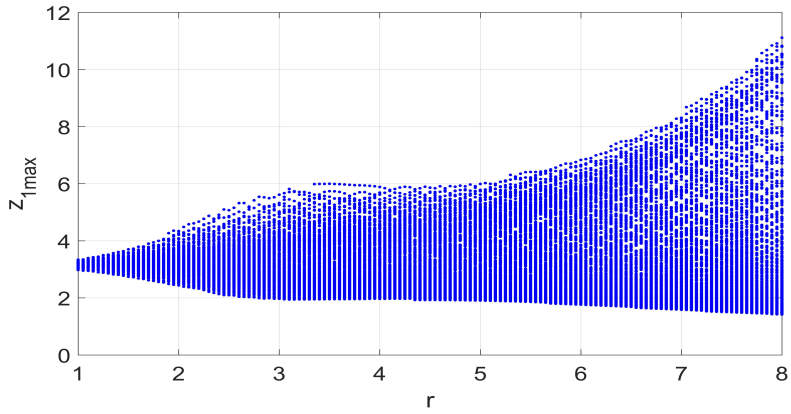

(a)

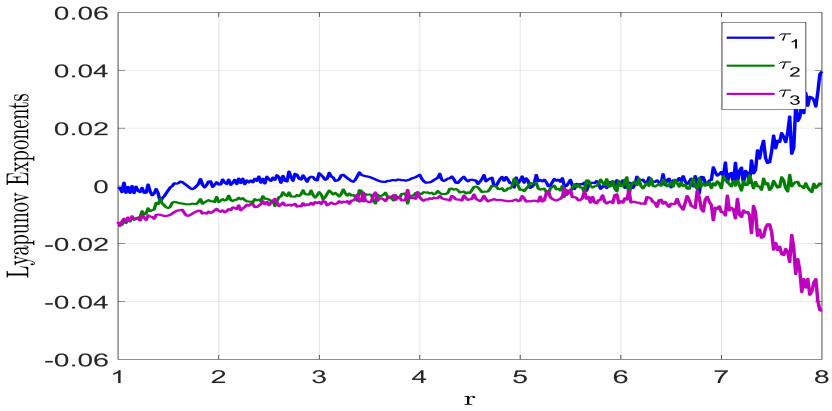

(b)

Figure 8: Dynamic analysis of the new 3-species population biology system (5) when $p = 1.8$, $q = 3$, $r \in [1, 8]$ and $s = 0.2$: (a) Bifurcation diagram and (b) LE spectrum

When $r \in [1, 2]$, the new population biology model (5) has one zero LE and two negative LEs indicating that it exhibits periodic behavior. In Figure 9(a), the (z_2, z_3) periodic attractor is plotted for $r = 1$. The associated Lyapunov exponents (LEs) and Kaplan-Yorke dimension (D_{KY}) are:

1) $\tau_1 = 0$, $\tau_2 = -0.014$ and $\tau_3 = -0.020$.

2) $D_{KY} = 0$.

As seen in Figure 8(b), the new population biology model (5) has one positive LE smaller than 0.01 for $r \in [2, 7.5]$. Hence, the system (5) exhibits weak chaotic behavior across this parameter r range. We select a value from this range, and we set r to be: $r = 4$. The (z_1, z_3) chaotic attractor of the system (5) is then presented in red for $r = 4$ as seen in Figure 9(b). The associated LEs and DKY are as follows:

1) $\tau_1 = 0.003$, $\tau_2 = 0$ and $\tau_3 = -0.004$.
2) $D_{KY} = 2.75$.

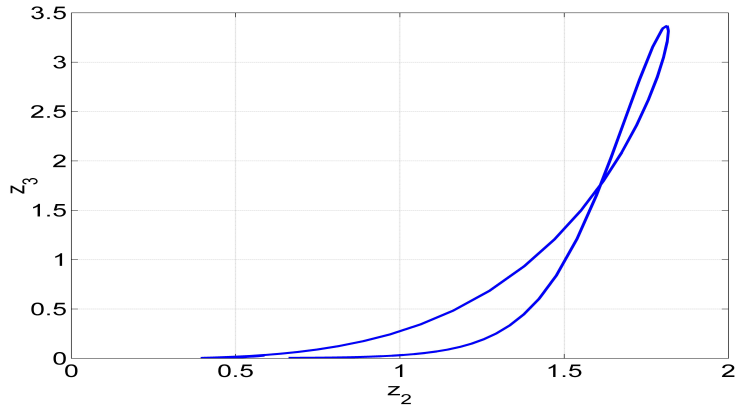

(a)

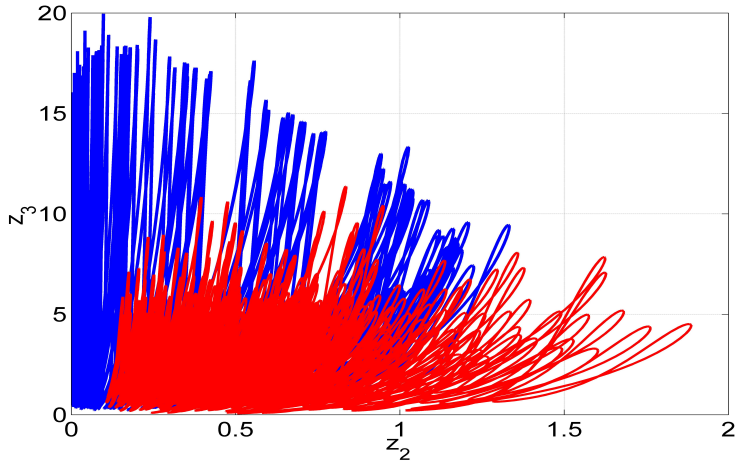

(b)

Figure 9: MATLAB phase portraits of the new population biology system (5) in (z_2, z_3) plane for different values of r: (a) Periodic attractor ($r = 1$) and (b) in blue: chaotic attractor ($r = 7.9$), in red: chaotic attractor ($r = 4$)

As seen in Figure 8(b), the new population biology model (5) has one positive LE bigger than 0.01 for $r \in [7.5, 8]$. Hence, the system (5) exhibits robust chaotic behavior across this parameter r range. We select a value from this range, and we set r to be: $r = 7.9$. The (z_1, z_3) chaotic attractor of the system (5) is then presented in blue for $r = 7.9$ as seen in Figure 9(b). The associated LEs and DKY are as follows:

1) $\tau_1 = 0.030$, $\tau_2 = 0$ and $\tau_3 = -0.036$.

2) $D_{KY} = 2.83$.

3.4. Variation of the parameter s

Here, we fix $p = 1.8$, $q = 3$, $r = 8$ and vary s in the interval $[0, 0.2]$.

Figure 10 represents the LEs spectrum and bifurcation diagram of system (5) when s increases from 0 to 0.2. It demonstrates how sensitive the new population biology system (5) is to variations in the parameter s value.

By examining the LEs and the bifurcation diagram shown in Figure 10, we find that the novel population biology model (5) may experience a set of scenarios, such as quasi-periodic attractor, weak chaotic attractor or robust chaotic attractor, depending on the value of parameter s.

When $s \in [0, 0.06]$, the new population biology model (5) has two zero LEs and one negative LE indicating that it exhibits quasi-periodic behavior. In Figure 11(a), the (z_1, z_2, z_3) quasi-periodic attractor of the system (5) is shown in green for $s = 0$. The associated Lyapunov exponents (LEs) and Kaplan-Yorke dimension (D_{KY}) are:

1) $\tau_1 = 0$, $\tau_2 = 0$ and $\tau_3 = -0.004$.

2) $D_{KY} = 0$.

As seen in Figure 10(b), the new population biology model (5) has one positive LE smaller than 0.01 for $s \in [0.060, 0.186]$. Hence, the system (5) exhibits weak chaotic behavior across this parameter s range. We select a value from this range, and we set s to be: $s = 0.1$. The (z_1, z_2, z_3) chaotic attractor of the system (5) is then presented in red for $s = 0.1$ as seen in Figure 11(b). The associated LEs and DKY are as follows:

1) $\tau_1 = 0.001$, $\tau_2 = 0$ and $\tau_3 = -0.006$.

2) $D_{KY} = 2.17$.

As seen in Figure 10(b), the new population biology model (5) has one positive LE bigger than 0.01 for $s \in [0.186, 2]$. Hence, the system (5) exhibits

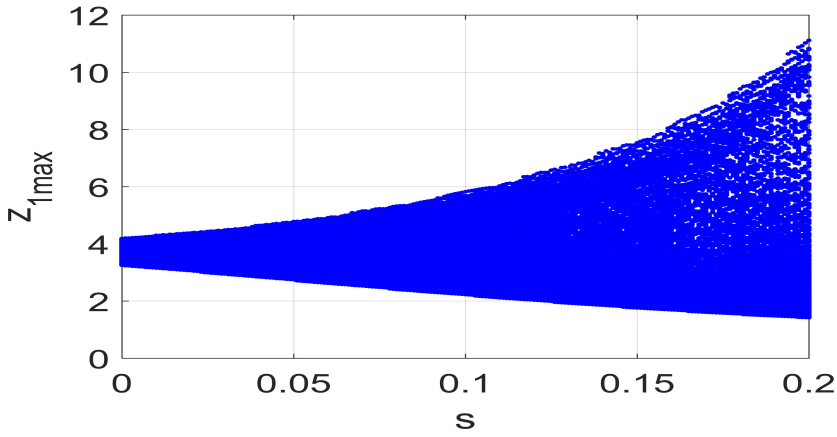

(a)

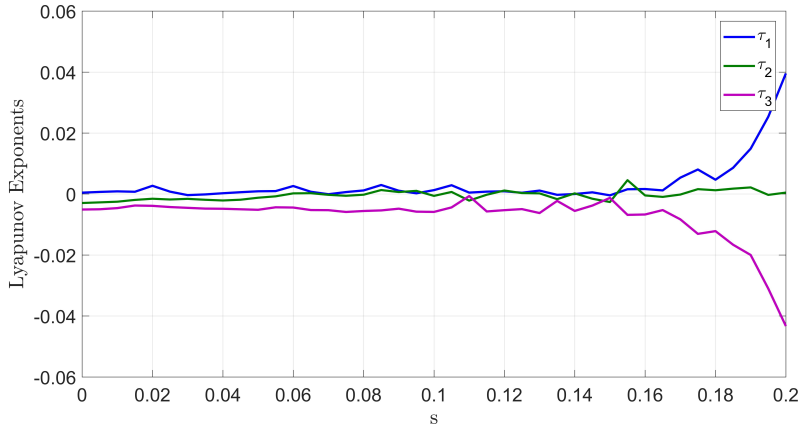

(b)

Figure 10: Dynamic analysis of the new 3-species population biology system (5) when $p = 1.8$, $q = 3$, $r = 8$ and $s \in [0, 0.2]$: (a) Bifurcation diagram and (b) LE spectrum

robust chaotic behavior across this parameter s range. We select a value from this range, and we set s to be: $s = 0.2$. The (z_1, z_2, z_3) chaotic attractor of the system (5) is then presented in blue for $s = 0.2$ as seen in Figure 11 (b). The associated LEs and DKY are as follows:

1) $\tau_1 = 0.039$, $\tau_2 = 0$ and $\tau_3 = -0.043$.

2) $D_{KY} = 2.91$.

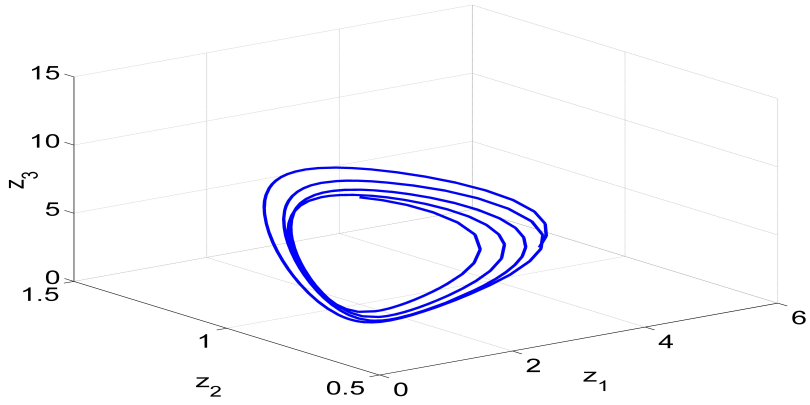

(a)

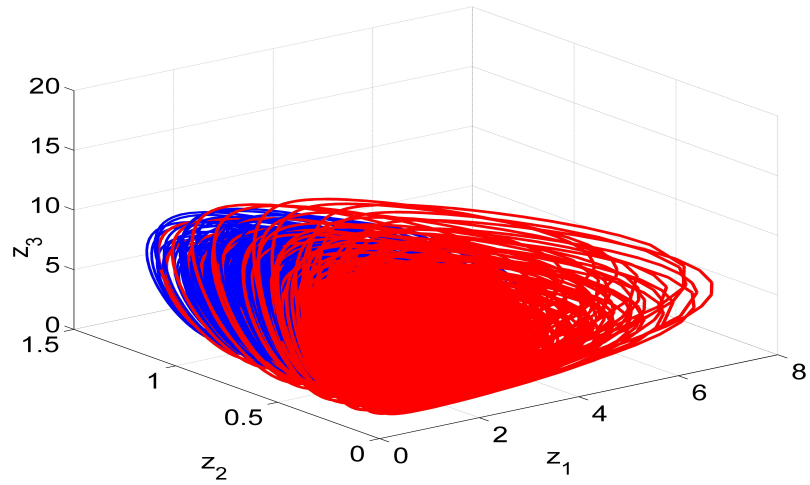

(b)

Figure 11: MATLAB phase portraits of the new population biology system (5) in (z_1, z_2, z_3) space for different values of s: (a) Quasi-periodic attractor ($s = 0$) and (b) in blue: chaotic attractor ($s = 0.2$), in red: chaotic attractor ($s = 0.1$)

3.5. Multistability with coexistence of chaotic attractors

For a chaotic dynamical system, multistability refers to the phenomenon of the coexistence of chaotic attractors for the same set of values of system constants but varying values of initial states of the system.

Figure 12 refers to the multistability of the new chaotic population biology system (5, showing the coexistence of two chaotic attractors for the same set of parameter values $(p, q, rs) = (1.8, 3, 8, 0.2)$ but different initial states, where the blue orbit corresponds to the initial state $Z_0 = (1.4, 1.0, 1.4)$ and the red orbit corresponds to the initial state $W(0) = (3.4, 1.0, 3.4)$.

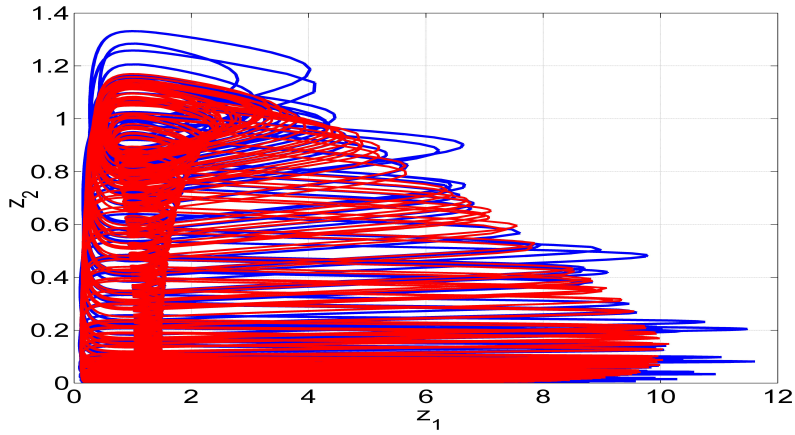

(a)

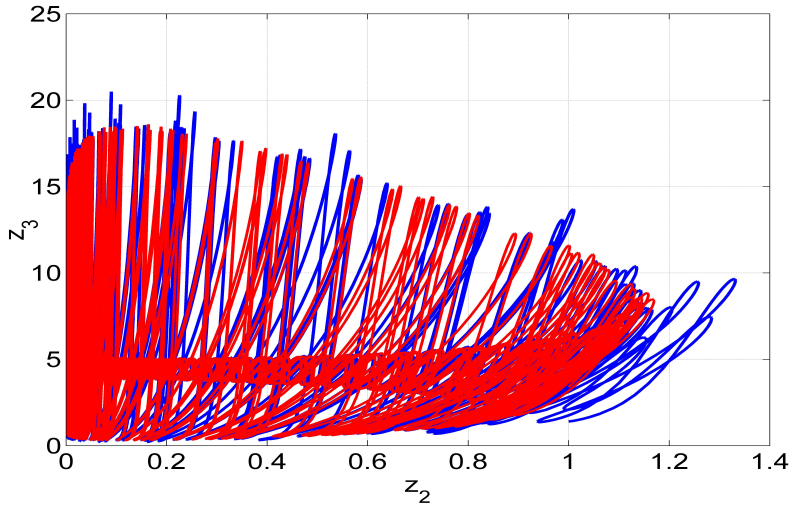

(b)

Figure 12: MATLAB phase portraits showing multistability with coexistence of chaotic attractors of the new chaotic population biology system (5), where the blue orbit corresponds to the initial state $Z_0 = (1.4, 1.0, 1.4)$ and the red orbit corresponds to the initial state $W(0) = (3.4, 1.0, 3.4)$

4. Master-slave synchronization of the new chaotic population systems

Integral sliding mode control (ISMC) is successfully deployed to achieve global asymptotic synchronization of the master chaotic population system (**M**) and slave chaotic population system (**S**).

$$(\mathbf{M}) \quad \begin{cases} \dot{z}_1 = z_1 - z_1 z_2 + r z_1^2 - s z_1 z_3 - p z_1^2 z_3 \,, \\ \dot{z}_2 = -z_2 + z_1 z_2 \,, \\ \dot{z}_3 = -q z_3 + s z_1 z_3 + p z_1^2 z_3 \,, \end{cases} \tag{9}$$

$$(\mathbf{S}) \quad \begin{cases} \dot{w}_1 = w_1 - w_1 w_2 + r w_1^2 - s w_1 w_3 - p w_1^2 w_3 + V_1 \,, \\ \dot{w}_2 = -w_2 + w_1 w_2 + V_2 \,, \\ \dot{w}_3 = -q w_3 + s w_1 w_3 + p w_1^2 w_3 + V_3 \,. \end{cases} \tag{10}$$

Here, V_1, V_2, V_3 are integral sliding mode controls (ISMC) which will be designed so as to synchronize the states of the master chaotic population system (M) and the slave chaotic population system (S).

The synchronization error between the chaotic population systems (M) and (S) is defined as follows:

$$\begin{cases} E_1 = w_1 - z_1 \,, \\ E_2 = w_2 - z_2 \,, \\ E_3 = w_3 - z_3 \,. \end{cases} \tag{11}$$

The error dynamics is obtained as follows:

$$\begin{cases} \dot{E}_1 = E_1 - w_1 w_2 + z_1 z_2 + r(w_1^2 - z_1^2) \\ \qquad - s(w_1 w_3 - z_1 z_3) - p(w_1^2 w_3 - z_1^2 z_3) + V_1 \,, \\ \dot{E}_2 = -E_2 + w_1 w_2 - z_1 z_2 + V_2 \,, \\ \dot{E}_3 = -q E_3 + s(w_1 w_3 - z_1 z_3) + p(w_1^2 w_3 - z_1^2 z_3) + V_3 \,. \end{cases} \tag{12}$$

With each error variable, we link an integral sliding surface as follows:

$$\begin{cases} S_1 = E_1 + m_1 \displaystyle\int_0^t E_1(\tau)\,\mathrm{d}\tau \,, \\ S_2 = E_2 + m_2 \displaystyle\int_0^t E_2(\tau)\,\mathrm{d}\tau \,, \\ S_3 = E s_3 + m_3 \displaystyle\int_0^t E_3(\tau)\,\mathrm{d}\tau \,. \end{cases} \tag{13}$$

By differentiation of the equations (13), we get

$$\begin{cases} \dot{S}_1 = \dot{E}_1 + \gamma_1 E_1 , \\ \dot{S}_2 = \dot{E}_2 + \gamma_2 E_2 , \\ \dot{S}_3 = \dot{E}_3 + \gamma_3 E_3 . \end{cases} \tag{14}$$

The integral sliding mode controls for the master-slave synchronisation are defined as follows:

$$\begin{cases} V_1 = -E_1 + w_1 w_2 - z_1 z_2 - r(w_1^2 - w_2^2) + s(w_1 w_3 - z_1 z_3) \\ \qquad + p(w_1^2 w_3 - z_1^2 z_3) - \gamma_1 E_1 - \alpha_1 \mathrm{sgn}(S_1) - \beta_1 S_1 , \\ V_2 = -\gamma_2 E_2 - \alpha_2 \mathrm{sgn}(S_2) - \beta_2 S_2 , \\ V_3 = qE_3 - s(w_1 w_3 - z_1 z_3) - p(w_1^2 w_3 - z_1^2 z_3) \\ \qquad - \gamma_3 E_3 - \alpha_3 \mathrm{sgn}(S_3) - \beta_3 S_3 . \end{cases} \tag{15}$$

By plugging in the sliding control law (15) into the error dynamics (12), we get

$$\begin{cases} \dot{E}_1 = -\gamma_1 E_1 - \alpha_1 \,\mathrm{sgn}(S_1) - \beta_1 S_1 , \\ \dot{E}_2 = -\gamma_2 E_2 - \alpha_2 \,\mathrm{sgn}(S_2) - \beta_2 S_2 , \\ \dot{E}_3 = -\gamma_3 E_3 - \alpha_3 \,\mathrm{sgn}(S_3) - \beta_3 S_3 . \end{cases} \tag{16}$$

Theorem 1 *The master-slave 3-D chaotic population models (9) and (10) are asymptotically and globally synchronised by the integral sliding mode control law (15) where γ_i, α_i, β_i, $(i = 1, 2, 3)$ are assumed to be positive constants.*

Proof. We define the Lyapunov function candidate as

$$V(S_1, S_2, S_3) = \frac{1}{2}\left(S_1^2 + S_2^2 + S_3^2\right) \tag{17}$$

which is obviously a positive definite function on $\mathbf{R}^3$.

We observe next that

$$\dot{V} = S_1 \dot{S}_1 + S_2 \dot{S}_2 + S_3 \dot{S}_3 . \tag{18}$$

Using (14) and (16), we simplify (18) as

$$\dot{V} = \sum_{i=1}^{3} S_i(-\alpha_i \,\mathrm{sgn}(S_i) - \beta_i S_i). \tag{19}$$

A simplification shows that

$$\dot{V} = -\sum_{i=1}^{3} \left[\alpha_i |S_i| + \beta_i S_i^2\right]. \tag{20}$$

Since $\alpha_i > 0$ and $\beta_i > 0$ for $i = 1, 2, 3$, we conclude that $\dot{V}$ is a strictly negative definite function defined on $\mathbf{R}^3$.

By Lyapunov stability theory, we have $S_i(t) \to 0$ for $i = 1, 2, 3$ as $t \to \infty$.

Consequently, we see that $E_i(t) \to 0$ for $(i = 1, 2, 3)$ as $t \to \infty$. □

For MATLAB simulations, the parameters of the 3-D population models are taken as in the chaotic case, *viz.* $p = 1.8$, $q = 3$, $r = 8$, and $s = 0.2$.

The sliding constants for numerical simulations are assumed as $\alpha_i = 0.3$, $\beta_i = 9$ and $\gamma_i = 12$ for $i = 1, 2, 3$.

For the master population system (M), the initial state is assumed as

$$z_1(0) = 4.2, \quad z_2(0) = 12.5, \quad z_3(0) = 7.1. \tag{21}$$

For the slave population system (S), the initial state is assumed as

$$w_1(0) = 14.1, \quad w_2(0) = 8.7, \quad w_3(0) = 11.6. \tag{22}$$

The time-history for the synchronization errors between the master system (M) and the slave system (S) is depicted in Figure 13.

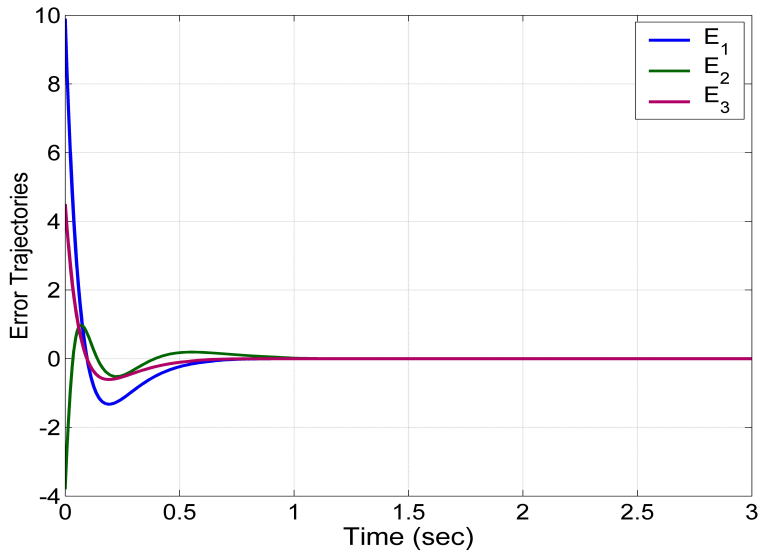

Figure 13: MATLAB plot of the time-trajectories of the synchronization errors between the master and slave chaotic population systems

From Figure 13, we can see that the master system (M) and the slave system (S) are quickly synchronised in our numerical simulation.

5. Circuit design of the new chaotic population biology system with one prey and two predators

The circuit design of the new chaotic population biology system (5) with one prey and two predators is given in Figure 14.

Electronic circuit implementation of the new population biology chaotic system is designed for the parameters $(p, q, r, s) = (1.8, 3, 8, 0.2)$ with initial conditions $Z(0) = (1.4, 1.0, 1.4)$. The designed circuit includes 2 analog multipliers (AD63JN), 7 operational ampliers (TL083CD), 17 resistors and 4 capacitors. For the circuit design, the the new population biology chaotic system has to be rescaled by using the following scaling of variables:

$$\begin{cases} Z_1 = \dfrac{1}{2}\, z_1 \,, \\ Z_2 = \dfrac{1}{2}\, z_2 \,, \\ Z_3 = \dfrac{1}{4}\, z_3 \,. \end{cases} \tag{23}$$

Replacing the new variables on the new population biology chaotic system (5), we obtain the following system:

$$\begin{cases} \dot{Z}_1 = Z_1 - 2Z_1Z_2 + 2rZ_1^2 - 4sZ_1Z_3 - 8pZ_1^2Z_3 \,, \\ \dot{Z}_2 = -Z_2 + 2Z_1Z_2 \,, \\ \dot{Z}_3 = -qZ_3 + 2sZ_1Z_3 + 4pZ_1^2Z_3 \,. \end{cases} \tag{24}$$

The circuit equation of the new chaotic population biology system after using Kirchhoff's electrical circuit laws can be derived as follows:

$$\begin{cases} C_1\dot{Z}_1 = \dfrac{1}{R_1}\, Z_1 - \dfrac{1}{R_2}\, Z_1Z_2 + \dfrac{1}{R_3}\, Z_1^2 - \dfrac{1}{R_4}\, Z_1Z_3 - \dfrac{1}{R_5}\, Z_1^2Z_3 \,, \\ C_2\dot{Z}_2 = -\dfrac{1}{R_6}\, Z_2 + \dfrac{1}{R_7}\, Z_1Z_2 \,, \\ C_3\dot{Z}_3 = -\dfrac{1}{R_8}\, Z_3 + \dfrac{1}{R_9}\, Z_1Z_3 + \dfrac{1}{R_{10}}\, Z_1^2Z_3 \,. \end{cases} \tag{25}$$

Here, Z_1, Z_2, Z_3 are the voltages across the capacitors C_1, C_2, C_3, respectively. We choose the values of the circuital elements as in Table 1.

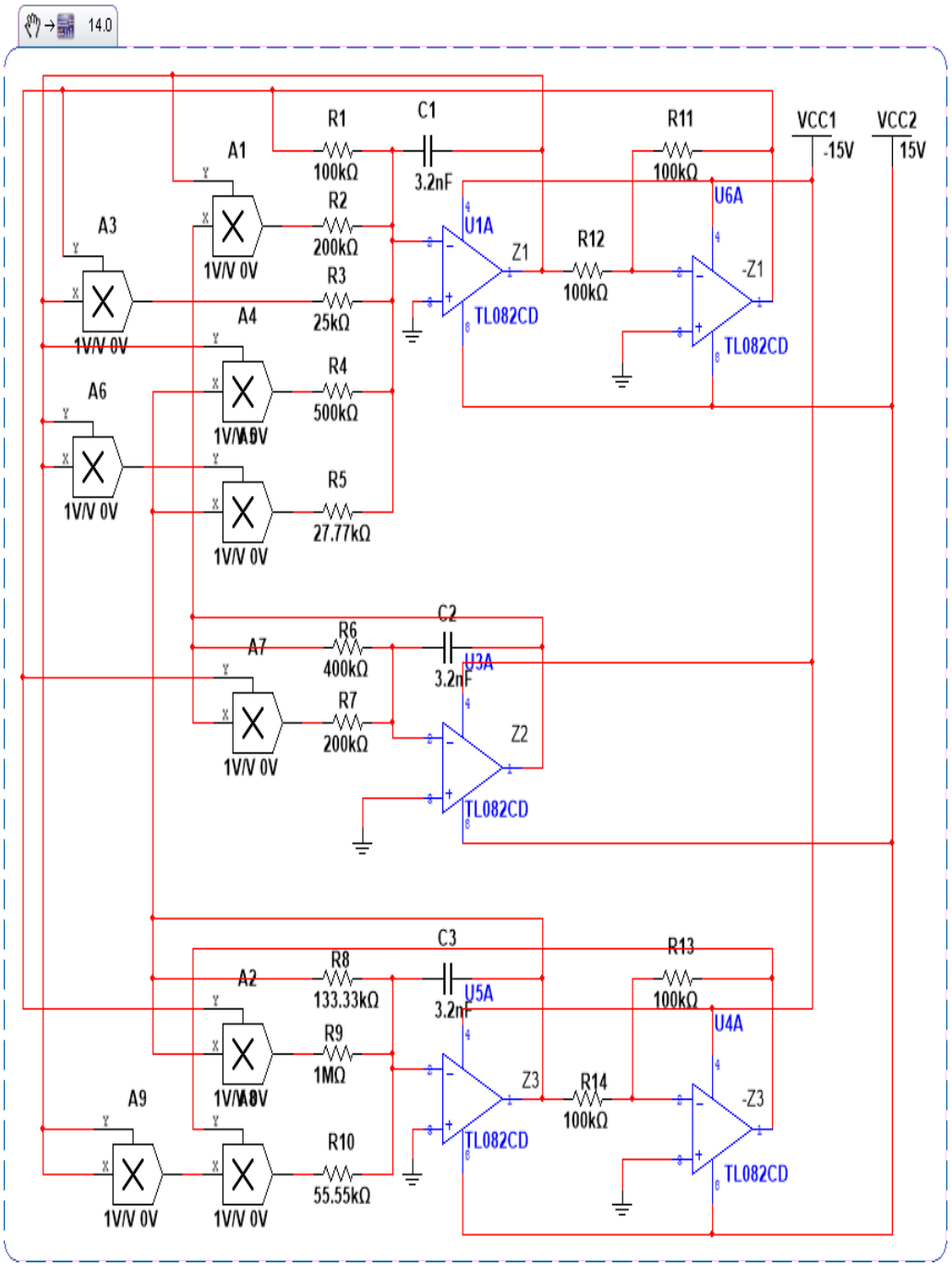

Figure 14: Circuit design of the new chaotic population biology system

Table 1: The Values of the Circuit Components in the 3-D Chaotic Circuit (25)

Circuit component	Value
R_1	100 kΩ
R_2, R_7	200 kΩ
R_4	500 kΩ
R_5	27.77 kΩ
R_6	400 kΩ
R_8	133.33 kΩ
R_9	1 mΩ
R_{10}	55.55 kΩ
$R_{11}, R_{12}, R_{13}, R_{14}$	100 kΩ
The power supplies	±15 Volts

With Multisim 14.0, we obtain the experimental observations of the new chaotic population biology system (25) as shown in Figures 15, 16 and 17. It can be seen that a good qualitative agreement between the MATLAB simulations of the new chaotic population system (5) and the Multisim simulations of the new chaotic population circuit system (25) is confirmed.

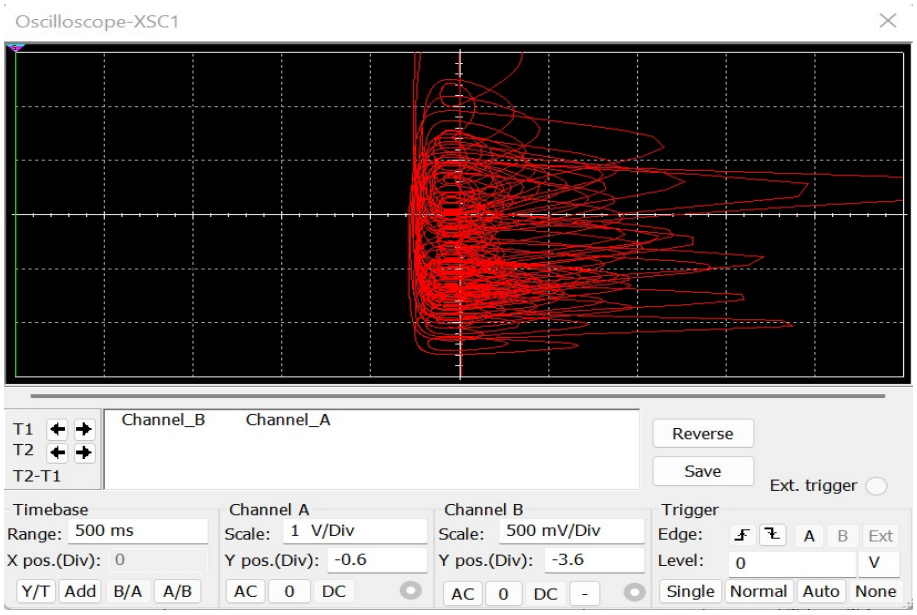

Figure 15: Circuit simulation using Multisim for the chaotic population circuit model (25) in the (Z_1, Z_2) plane

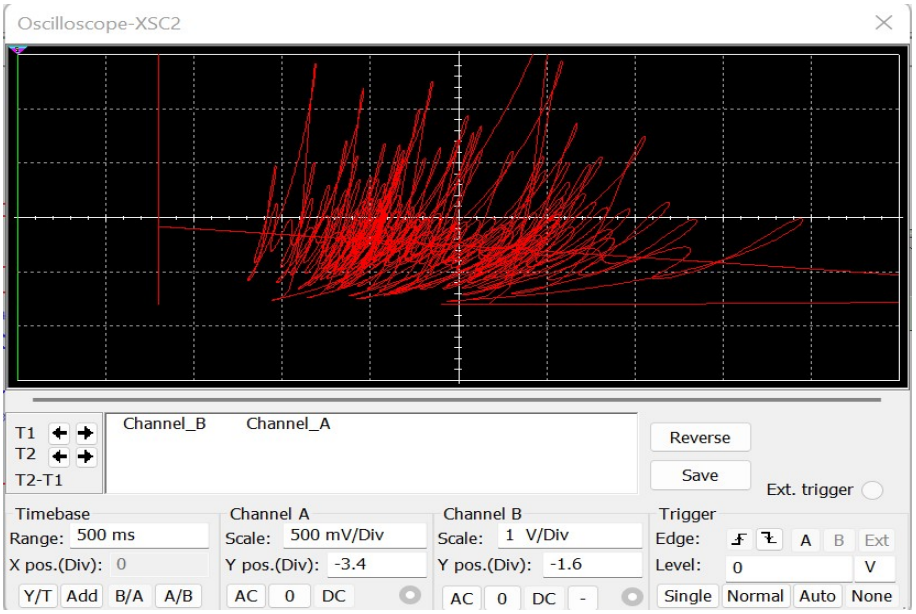

Figure 16: Circuit simulation using Multisim for the chaotic population circuit model (25) in the (Z_2, Z_3) plane

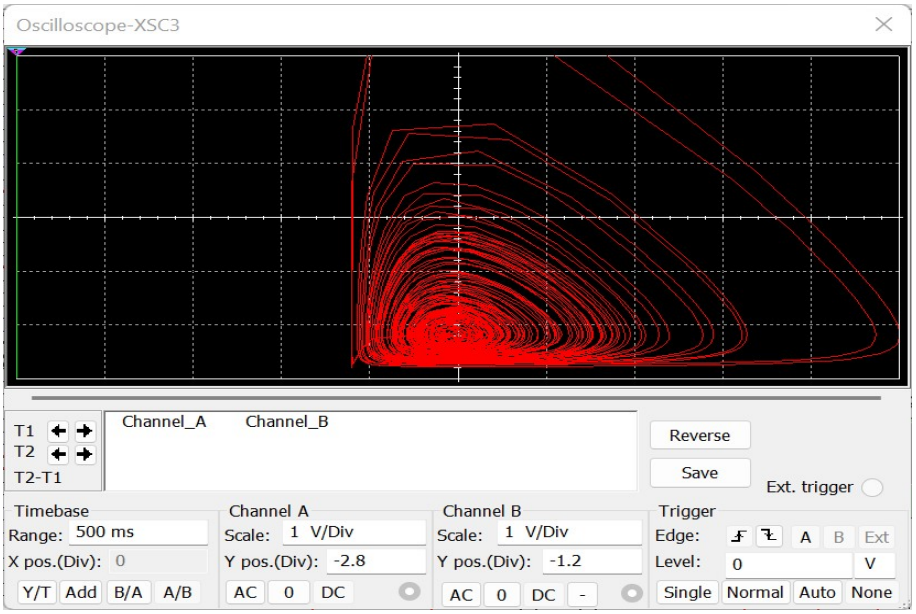

Figure 17: Circuit simulation using Multisim for the chaotic population circuit model (25) in the (Z_1, Z_3) plane

6. Conclusions

We reported a new chaotic population biology system with one prey and two predators. Our new chaotic population model was basically derived by means of introducing two nonlinear interaction terms between the prey and predator-2 to the Samardzija-Greller population biology system (1988). We established that the new chaotic population biology system has a greater value of Maximal Lyapunov Exponent (MLE) than the Maximal Lyapunov Exponent (MLE) of the Samardzija-Greller population biology system (1988). We carried out a detailed bifurcation analysis of the new chaotic population biology system with one prey and two predators. We also established that the new chaotic population biology model exhibits multistability with coexisting chaotic attractors. Next, we applied integral sliding mode control for the complete synchronization of the new chaotic population biology system with itself, taken as the master and slave chaotic population biology systems. MATLAB simulations were shown to illustrate the phase orbits of the new chaotic population model, bifurcation analysis of the new chaotic population model and the control results via sliding mode control. Finally, for the practical use of the new chaotic population biology system, we designed an electronic circuit design using MultiSim (Version 14.0).

References

[1] L. Liu and J. Wang: A cluster of 1D quadratic chaotic map and its applications in image encryption. *Mathematics and Computers in Simulation*, **204** (2023), 89–114. DOI: 10.1016/j.matcom.2022.07.030.

[2] K. Cao and Q. Lai: A simple memristive chaotic system with complex dynamics and ITS image encryption application. *International Journal of Modern Physics B*, **36**(21), (2022). DOI: 10.1142/S0217979222501314.

[3] C. Xiu, J. Fang, and X. Ma: Design and circuit implementations of multi-memristive hyperchaotic system. *Chaos, Solitions and Fractals*, **161** (2022). DOI: 10.1016/j.chaos.2022.112409.

[4] Y. Wang, H. Li, Y. Guan, and M. Chen: Predefined-time chaos synchronization of memristor chaotic systems by using simplified control inputs. *Chaos, Solitions and Fractals*, **161** (2022). DOI: 10.1016/j.chaos.2022.112282.

[5] N. Abbassi, M. Gafsi, R. Amdouni, M.A. Hajjaji and A. Mtibaa: Hardware implementation of a robust image cryptosystem using reversible cellular-automata rules and 3-D chaotic systems. *Integration*, **87** (2022), 49–66. DOI: 10.1016/j.vlsi.2022.06.007.

[6] L. Minati, J. Bartels, C. Li, M. Frasca, and H. Ito: Synchronization phenomena in dual-transistor spiking oscillators realized experimentally towards physical reservoirs. *Chaos, Solitions and Fractals*, **162** (2022). DOI: 10.1016/j.chaos.2022.112415.

[7] I. Mishra, S. Jain, and V. Maik: Secured ECG signal transmission using optimized EGC with chaotic neural network in WBSN. *Computer Systems Science and Engineering*, **44**(2), (2022), 1109–1123. DOI: 10.32604/csse.2023.025999.

[8] P. Tao, J. Cheng, and L. Chen: Brain-inspired chaotic backpropagation for MLP. *Neural Networks*, **155** (2022), 1–13. DOI: 10.1016/j.neunet.2022.08.004.

[9] G. Arthi, V. Thanikaiselvan and R. Amirtharajan: 4D hyperchaotic map and DNA encoding combined image encryption for secure communication. *Multimedia Tools and Applications*, **81**(11), (2022), 15859–15878. DOI: 10.1007/s11042-022-12598-5.

[10] P. Ramadevi, T. Jayashankar, V. Dinesh, and M. Dhamodaran: Chaotic sandpiper optimization based virtual machine scheduling for cyber-physical systems. *Computer Systems Science and Engineering*, **44**(2), (2022), 1373–1385. DOI: 10.32604/csse.2023.026603.

[11] A.J. Lotka: *Elements of Physical Biology*. Williams and Wilkins, Philadelpha, USA, 1925.

[12] V. Volterra: Variazioni e fluttuazioni del numero d'individui in specie animali conviventi. *Memoria della Reale Accademia Nazionale dei Lincei*, **2** (1926), 31–113.

[13] N. Samardzija and L.D. Greller: Explosive route to chaos through a fractal torus in a generalized Lotka-Volterra model. *Bulletin of Mathematical Biology*, **50**(5), (1988), 465–491.

[14] S.K. Agrawal, M. Srivastava, and S. Das: Synchronization between fractional-order Ravinovich-Fabrikant and Lotka-Volterra systems. *Nonlinear Dynamics*, **69** (2012), 2277–2288. DOI: 10.1007/s11071-012-0426-y.

[15] M.F. Danca and G. Chen: Bifurcation and chaos in a complex model of dissipative medium. *International Journal of Birucation and Chaos*, **14**(10), (2004), 3409–3447. DOI: 10.1142/S0218127404011430.

[16] U.E. Kocamaz, A. Goksu, H. Taskin, and Y. Uyaroglu: Control of chaotic two-predator one-prey model with single state control signals. *Journal of Intelligent Manufacturing*, **32** (2021), 1563–1572. DOI: 10.1007/s10845-020-01676-w.

[17] J. Xing, Z. Yang, and Y. Ren: Analysis of bifurcation and chaotic behavior for the flexspline of an electromagnetic harmonic drive system with movable teeth transmission. *Applied Mathematical Modelling*, **112** (2022), 467–485. DOI: 10.1016/j.apm.2022.07.007.

[18] H. Zhou and L. Yang: Dynamical analysis arising from the Willamowski-Rössler model. *Journal of Mathematical Analysis and Applications*, **514**(2), (2022), DOI: 10.1016/j.jmaa.2022.126281.

[19] S. Contreras-Celada, M.G. Cleric, S. Coulibaly, R.G. Rojas, and A.O. Leon: Voltage-driven multistability and chaos in magnetic films. *Journal of Magnetism and Magnetic Materials*, **562** (2022). DOI: 10.1016/j.jmmm.2022.169793.

[20] Z. Wang, F. Parastesh, H. Tian, and S. Jafari: Symmetric synchronization behavior of multistable chaotic systems and circuits in attractive and repulsive couplings. *Integration*, **89** (2023), 37–46. DOI: 10.1016/j.vlsi.2022.11.007.

[21] S. Vaidyanathan, A.T. Azar, A. Akgul, C.H. Lien, S. Kacar, and U. Cavusoglu: A memristor-based system with hidden hyperchaotic attractors, its circuit design, synchronisation via integral sliding mode control and an application to voice encryption. *International Journal of Automation and Control*, **13**(6), (2019), 644–667. DOI: 10.1504/IJAAC.2019.102665.

[22] S. Vaidyanathan, L.G. Dolvis, K. Jacques, C.H. Lien, and A. Sambas: A new five-dimensional four-wing hyperchaotic system with hidden attractor, its electronic circuit realisation and synchronisation via integral sliding mode control. *International Journal of Modelling, Identification and Control*, **32**(1), (2019), 30–45. DOI: 10.1504/IJMIC.2019.101959.

[23] S. Vaidyanathan and A. Rhif: A novel four-leaf chaotic system, its control and synchronisation via integral sliding mode control. *International Journal of Modelling, Identification and Control*, **28**(1), (2019), 28–39. DOI: 10.1504/IJMIC.2017.085295.

[24] K. Karawanich and P. Prommee: High-complex chaotic system based on new nonlinear function and OTA-based circuit realization. *Chaos, Solitons and Fractals*, **162** (2022). DOI: 10.1016/j.chaos.2022.112536.

[25] Q. Guo, N. Wang, and G. Zhang: A novel four-element RCLM hyperchaotic circuit based on current-controlled extended memristor. *AEU – International Journal of Electronics and Communications*, **156** (2022). DOI: 10.1155/2021/5582774.